

# Integration of bioenergetics in an Individual Based Model to hindcast anchovy dynamics in the Bay of Biscay

Juan Bueno-Pardo<sup>1\*</sup>, Pierre Petitgas<sup>2</sup>, Susan Kay<sup>3</sup>, Martin Huret<sup>1</sup>

\* Corresponding author: [jbuenopardo@gmail.com](mailto:jbuenopardo@gmail.com)

1. Ifremer, STH/LBH, BP 70, Plouzané 29280, France

2. Ifremer, EMH, rue de l'Île d'Yeu, BP 21105, 44311 Nantes Cedex 3, France

3. Plymouth Marine Laboratory, Prospect Place, The Hoe, Plymouth PL1 3DH, United Kingdom

KEYWORDS: anchovy, Dynamic Energy Budget, Individual Based Model, Bay of Biscay, fishery, population collapse, Harvest Control Rule

Declarations of interest: none

## 20 Abstract

22 The population of European anchovy of the Bay of Biscay collapsed at the beginning of the 21<sup>st</sup>  
century, causing the closure of its fishery between 2005 and 2010. In order to study both the  
human and environmental causes of the anchovy population dynamics, an approach coupling  
24 individual bioenergetics to an individual-based model was applied between 2000 and 2015. This  
modelling framework was forced with outputs from a physical-biogeochemical model. In addition  
26 to a base-case scenario with realistic forcing, alternative scenarios were run without interannual  
variability in either fishing mortality or environmental conditions. During the decrease in  
28 population biomass, a high fishing pressure coincided with a combination of environmental  
variables promoting the appearance of large individuals that could not survive severe winters  
30 because of their high energetic demands. The recovery of the population was favoured by a  
period of warm years with abundant food favouring the winter survival of age 1 individuals, in  
32 coincidence with the closure of the fishery. Our modelling approach also allows to test the  
consequences of a retrospective implementation of the current harvest control rule from 2000  
34 which, according to our results, would have prevented the collapse of the population and  
avoided the fishery closure.

36

## Introduction

Like other small pelagic fish with a short lifespan, early maturation and high reproductive potential, the European anchovy (*Engraulis encrasicolus*) plays a pivotal ecological role due to its intermediate trophic position, high abundance, and energy content (Cury et al., 2000; Palomera et al., 2007). The population dynamics of small pelagic fish are often abrupt and tightly tied to environmental features by complex relationships (Checkley et al., 2009). Environmental forcing is known to affect population dynamics through both biological (e.g. changes in life history traits, physiological optima, behaviour, etc.) and physical (e.g. affecting survival, larval dispersion, feeding, etc.) pathways (Checkley et al., 2009).

In the Bay of Biscay (NE Atlantic), the anchovy population sustains a valuable fishery shared by France and Spain. The historical evolution of landings of anchovy peaked between 1960 and 1965, with ca. 75,000 tonnes per year, while minimal landings occurred at the beginning of the 21<sup>st</sup> century (ICES, 2018). In 2005, the population reached a historical minimum that forced the closure of the fishery between 2005 and 2010, entailing important socio-economic consequences (Vermard et al., 2008). The effect of fishing and environmental variables has been widely studied to understand both the drivers of this population and the causes of its collapse and, although a wide variety of approaches have been applied in this regard, few have succeeded in understanding the underlying biological or ecological mechanisms.

The literature on the effects of fishing and environment on the populations of small pelagic fish typically considers two levels of biological organization: populations and individuals (physiology). Among the first group, time-series correlation analyses have been used with different results. Hence, while the anchovy recruitment was not found to be related to zooplankton concentration (Irigoien et al., 2009), the East-Atlantic oscillation index successfully explained part of the recruitment failure at the beginning of the 21<sup>st</sup> century (Borja et al., 2008). Similarly, recruitment was found to be positively and negatively correlated to the magnitude of coastal upwelling and the degree of shelf stratification respectively (Allain et al., 2001). Other studies found that larval survival was related to anchovy spawning distribution (Allain et al., 2007). Using a Bayesian approach, Taboada and Anadón (2016) showed that changes in phytoplankton phenology and larval drift presented good prediction indicators for the dynamics of the population but, to explain the collapse of the population, fishing pressure needed to be

considered, improving considerably the skill of the models. At the individual/physiological level, several studies tried to determine the effect of environmental variables on life history traits such as growth (Cotano et al., 2008), mortality rates (Cotano et al., 2008; Uriarte et al., 2016) or reproduction (Motos, 1996; Somarakis et al., 2004). As far as we know, none of the previous works developed a mechanistic approach linking the effect of environmental conditions to the response of the population based on the physiology of individuals.

The Dynamic Energy Budget theory (DEB; Kooijman, 2010) is a metabolic-ecology theory describing the acquisition, use, and distribution of energy by individuals through metabolic reactions. In DEB theory, the energy from the environment is allocated through assimilation into three different compartments: structure, maintenance and reproduction/maturation, while temperature controls the velocity of all the metabolic reactions and fluxes of energy within the organism. Hence, the DEB theory facilitates understanding of the relationships between an individual's energy and life history traits such as growth, reproduction, and mortality rates. A model based on the DEB theory has recently been assembled for the anchovy in the Bay of Biscay, describing its bioenergetics at annual and life-cycle scales (Gatti et al., 2018). These kind of bioenergetic approaches are also useful to compare the life histories of individuals among geographic regions (Huret et al., 2018), and for understanding the variations in vital rates found in response to environmental fluctuations (Pethybridge et al., 2013; Politikos et al., 2015a; Politikos et al., 2015b). Integrating the information from different individuals, DEB models can further be scaled up to the population level using individual-based population models (IBMs, see Huse et al., 2002). The use of IBMs to infer the consequences of environmental changes on small pelagic fish populations has grown since the 1990's (e.g. Letcher et al., 1996; Rose et al., 1999,) but it was only after the inclusion of the full life cycle of fish (e.g. Jakobsen et al., 2009) that IBMs succeeded in capturing the effect of environmental variables on aspects such as reproduction and mortality (e.g. Fietcher et al., 2015; Politikos et al., 2018). In the case of anchovy, a plankton feeder, models considering low trophic levels (physical-biogeochemical models) provide the energy from the environment in the form of food (plankton) and temperature. In this manner, life history traits such as growth, reproduction, mortality or movement can be related to the environmental variables and, integrating these phenomena over an entire population, the response of the population can be simulated (Pethybridge et al., 2013, Politikos et al., 2015a).

In this work, we integrate the bioenergetics of individual anchovies, using a DEB model forced

with the outputs of a coupled physical-biogeochemical model, into a population (IBM) model, in  
104 order to create a unique mechanistic framework enabling us to understand the causes of the  
rapid collapse and slow recovery of the population between 2000 and 2015. This approach goes  
106 a step beyond the historical complexity of models for anchovy in the Bay of Biscay, and is used  
to study the human and environmental effects on anchovy dynamics, by simulating different  
108 scenarios of environmental and fishing pressures. Finally, the implementation of the current  
harvest control rule from the beginning of the century is simulated, in order to test whether this  
110 measure could have prevented the collapse of the population between 2005 and 2010.

112

## Materials and methods

In order to scale up the effect of environmental variables on the anchovy's bioenergetics and evaluate the response at the population level, a joint modelling framework consisting of a DEB model and an IBM was assembled (Fig. 1). This approach used the outputs (temperature and zooplankton concentration) from a regional physical-biogeochemical model as forcing for the DEB model for the anchovy described in Gatti et al. (2017). Then, an IBM integrated the response of the different individuals considered within the population (in terms of growth, reproduction, and mortality), to infer the evolution of the population over time (Fig. 1). In this section we describe in more detail the different modules, parameters and processes considered.

### Environmental forcing

The environmental forcing was provided by the regional coupled physical-biogeochemical POLCOMS-ERSEM model (Holt et al., 2001; Butenschön et al., 2016), using a 0.1° spatial resolution and 40 sigma layers over the period 1996-2015. The model was forced using reanalysis for the atmospheric interface (ERAinterim, Dee et al. 2011) and physical ocean boundary conditions (GLORYS2v4, product GLOBAL\_REANALYSIS\_PHY\_001\_025 from marine.copernicus.eu), with the biogeochemical boundary conditions and river inputs set using climatology (World Ocean Atlas, [www.nodc.noaa.gov/OC5/woa13/](http://www.nodc.noaa.gov/OC5/woa13/)), GLODAPv2 (<https://www.nodc.noaa.gov/ocads/oceans/GLODAPv2/>), and GlobalNEWS2 (Mayorga et al., 2010). Temperature (°C) and zooplankton biomass (mg C m<sup>-3</sup>) outputs of this model were used to force the DEB-IBM model. Our model is not spatially explicit, so the forcing variables were averaged over the Bay of Biscay region from the coast to 48.0° N and 5.0° W (Fig. 2 and Figs. S1-S4), which covers the distribution of the population over its life-cycle. The depth considered for the temperature series was integrated between 0 and 150 m for adults, and between 0 and 30 m for eggs, larvae and juveniles (Gatti et al., 2017), while the concentration of zooplankton in the first 50 m was used for the food density (Plounevez and Champalbert, 1999). Zooplankton biomass ( $X$ , mg C m<sup>-3</sup>) was then introduced as food concentration in the DEB model, being used to calculate the “scaled functional response” for food ( $f$ ) as a Holling type II function  $f = X / (X + K_f)$  (where  $K_f$  is the half saturation coefficient for food, see Table S1).

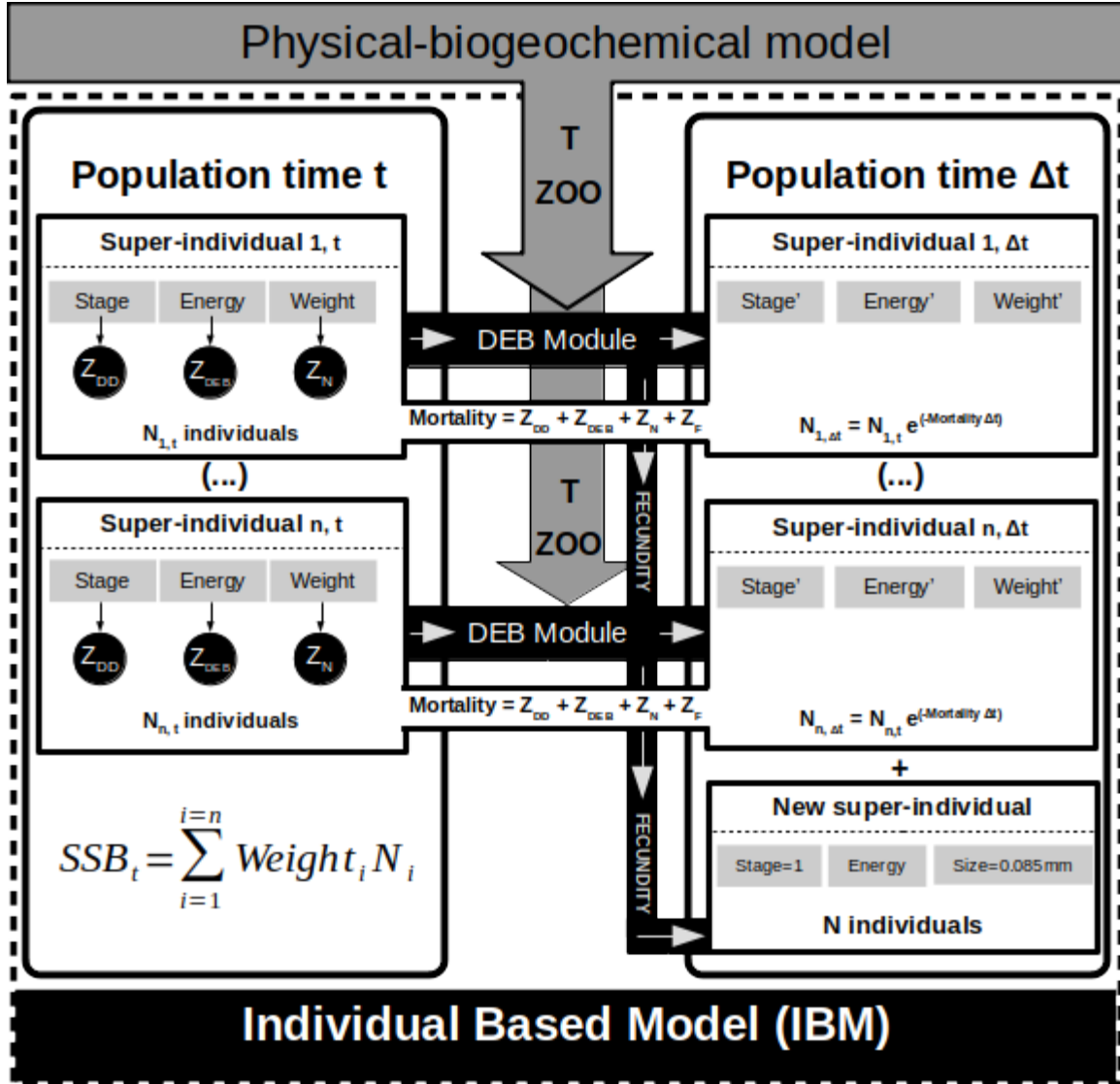


**Figure 1.** Schematic showing the integration of the population (IBM) and individual (DEB) modules over two consecutive time steps ( $t$  and  $\Delta t$ ). We consider  $n$  super-individuals per time step, with  $n$  varying each  $\Delta t$  due to mortality ( $z$ ) and fecundity. Temperature ( $T$ ) and zooplankton concentration ( $ZOO$ ) are provided by a regional physical-biogeochemical model that forces the bioenergetics of each super-individual (DEB module), making them change over time. Reproduction events can occur every 3 days between April and September. A super-individual disappears when all its individuals are dead. For each reproductive event, a new super-individual is created, being the sum of all the eggs spawned by the whole set of individuals of the population its initial number of individuals. Mortality sources correspond to  $Z_{DEB}$ : energetic failure (inability to allocate the required energy to maintenance);  $Z_N$ : natural mortality (related to body size, which is calculated from body weight, as described in Eq. 1) ;  $Z_F$ : fishing mortality (obtained from the literature, constant value per semester);  $Z_{DD}$ : density-dependent larval mortality (only applied to the larval stage and dependent on the estimated concentration of eggs, as described by Somarakis and Nikolioudakis, 2007, see Eq. 2).

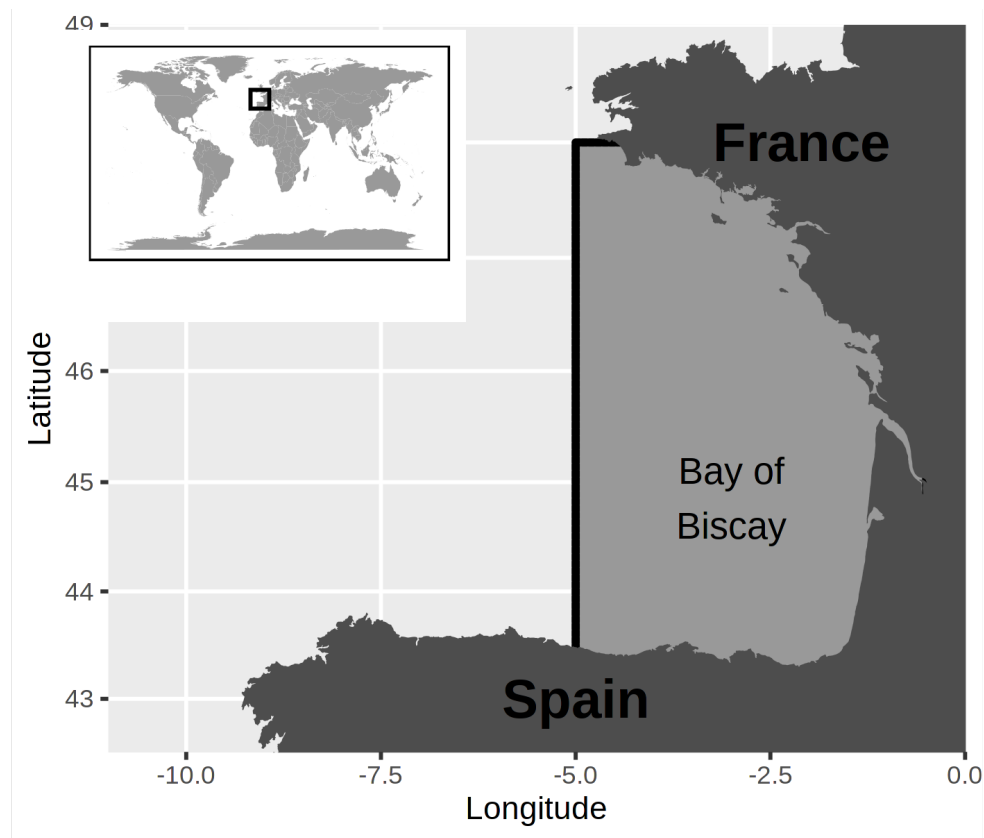


**Figure 2.** Location of the Bay of Biscay and the geographical extent considered in the analysis (grey area).

162

### Individual bioenergetics modelling

164 The anchovy life cycle was described by means of a bioenergetic model based on the Dynamic  
 Energy Budget (DEB) theory of Kooijman (2010) (DEB module). The values of the different  
 166 parameters considered in this model are shown in Table S1, while the equations describing the  
 main processes of the individual metabolism are presented in Table S2. Forcing the DEB  
 168 module with a physical-biogeochemical model for the Bay of Biscay (Fig. 2) makes it possible to  
 evaluate the impact of environmental variables on metabolic-dependent processes at the  
 170 individual level such as growth, fecundity or mortality.

172 The DEB module used here was calibrated for the Bay of Biscay anchovy by Gatti et al. (2017).



A simulation at the individual level using a daily environmental climatology of temperature and zooplankton from the period 1996-2015 ("individual run", Fig. S5), gave similar results to those of Gatti et al. (2017). However, because the coupled physical-biogeochemical model used as forcing was not the same than in their study, some minor adjustments to the maximum assimilation rate ( $p_{Am}$ ) and the fraction of energy allocated to growth ( $k$ ) were made (from 800 to 820 J cm<sup>-2</sup> d<sup>-1</sup>, and from 0.71 to 0.80 respectively).

## Population modelling

The DEB module was coupled to an individual based model (IBM). Super-individuals (SIs) were used as modelling units (Scheffer et al., 1995; Rose et al., 2015), in which each SI represented a large number of individuals born the same day and with identical life history and parameters. We integrated over all SIs to scale-up the response to environmental factors at the population level (IBM module). This consisted of the addition of the processes and state variables of the individuals forming each SI across the population (i.e. fecundity, biomass, growth, mortality, etc.), to infer the characteristics of the whole population. The population was initialised on April 1<sup>st</sup> 1996 and the model was run until December 31<sup>st</sup> 2015, with years 1996 to 1999 used as a 'spin-up' period to stabilize the population in terms of SI number. The initial number of individuals within each parental SI was derived from the age-structured data obtained in PELGAS surveys (Doray et al., 2018), while their size (g) and energy content on each of the DEB compartments (structural, reserve, and reproductive) were obtained from the individual run (Fig. S5). On this basis, the model started on April 1<sup>st</sup> 1996 with four adult SIs comprising different numbers of individuals ( $3.7 \times 10^9$ ,  $1.5 \times 10^9$ ,  $3.6 \times 10^8$ ,  $2.4 \times 10^7$ , respectively), with different age (1, 2, 3, 4 years, respectively), size (12.13, 16.20, 17.21, 17.56 cm, respectively), and energy in the different compartments of the DEB models: structure (20625, 45958, 50914, 58395 J, respectively), and reserve buffer (7548, 20676, 26693, 34644 J, respectively). The energy of the reproductive buffer was the same for each initial SI: 12026 J. The SIs were allowed to spawn every 3 days between April and September, creating new generations of SI during the "spin-up" period. All eggs spawned within 3 days by all adult SI were gathered in a unique new SI. The population variability in the model is generated by the effect of the different environmental variables experienced by SIs born at different moments of the year. In this manner, a pool of life histories during the spin-up period was originated, giving rise to a diversified population of 130 SIs on January 1<sup>st</sup> 2000, when the calibration period started (see below). The frequency for creating new SIs, which in turn controls the number of SIs in the model, was subject to a sensitivity analysis prior to the simulations. The objective was to find the

lowest number of SIs which allowed faster simulations without effects on the model results, i.e. allowing enough variability to be simulated based on the different life history trajectories of each SI.

Four sources of mortality were considered within the DEB-IBM framework. These mortalities are dependent on the energetic requirements, size, and stage of the fish, while the fishing mortality is considered as an external (fixed by semester) source of mortality. The mortality by energetic deprivation ( $Z_{DEB}$ ) is explicitly included in the DEB module. It occurs when a fish cannot supply the required energy for somatic maintenance costs, neither from its reserve or from emergency maintenance processes (reallocation from reproduction). This kind of mortality essentially occurs in late winter within our model in the Bay of Biscay.

Second, the natural mortality ( $Z_N$ ) considers implicitly the effects of predation and decreases with individual size (Fig. S6):

$$Z_N = Z_a + (Z_e - Z_a) e^{-z(L_T - L_{egg})} \quad \text{Eq. 1}$$

with  $Z_a$  and  $Z_e$  the instantaneous mortality rate of adults and eggs respectively, and  $z$  a decreasing coefficient of natural mortality.  $L_T$  is the individual length at a given time, and  $L_{egg}$  is the average size of an anchovy egg in the Bay of Biscay (0.0854 cm, Huret et al., 2016). These parameters ( $Z_a$ ,  $Z_e$ , and  $z$ ) are optimized during the calibration process (see below).

The third source of mortality is a density-dependent relationship between egg concentration and larval mortality established following the relationship by Somarakis and Nikolioudakis (2007) set in the Aegean Sea (Fig. S6):

$$Z_{DD} = -0.154 + \log(A) \quad \text{Eq. 2}$$

with  $Z_{DD}$  the larval density-dependent mortality (applied until individual size = 2.81 cm, Fig. S6) and  $A$  the concentration of eggs, expressed in number  $m^{-2}$  (we considered 50,000  $km^2$ , more or less half of the area of study, representing the potential spawning area of anchovy). The value of the slope ( $s = 0.205$ , according to Somarakis and Nikolioudakis, 2007) was also optimized during the calibration process (see below).

Finally, the fishing mortality ( $Z_F$ , Fig. S6) was introduced as a constrained external parameter with an updated value for every semester between 2000 and 2015 (data from ICES, 2018). Fishing mortality is considered as:

$$N_{t+\Delta t} = N_t e^{(-Z_F \Delta t)} \quad \text{Eq. 3}$$

where  $N_t$  and  $N_{t+\Delta t}$  are the fish abundances at time  $t$  and  $t+\Delta t$  respectively, being  $\Delta t$  the length of time step (1 hour). This mortality rate was applied to adults and juveniles (not yet matured) during the first semester of the year, and to actively reproducing adult individuals during the second semester of the year.

## Model calibration with optimization of mortality parameters

The outputs from a Bayesian two-stage biomass-based model (CBBM, Ibaibarriaga et al., 2008) were considered as reference for anchovy biomass in the Bay of Biscay between 2000 and 2015. These estimations are provided for the 1<sup>st</sup> of January. CBBM is the standard population assessment provided by ICES and considers two kinds of individuals in the population: adults participating in reproduction (spawning stock biomass, SSB), and recruits (age 1 adults that do not participate in reproduction). 1<sup>st</sup> January biomass values were obtained from the model based on individual weight, the total number of individuals, and their age. The differences between the outputs of the IBM model and the CBBM model were then computed as a cost function:

$$\sum_i \sum_y \left( \frac{B_{i,y} - B'_{i,y}}{\sigma_i} \right) \quad \text{Eq. 4}$$

where  $B_{i,y}$ , and  $B'_{i,y}$ , are the simulated and observed (CBBM) biomass of class  $i$  (SSB and recruits) respectively at time  $y$  (year), and  $\sigma_i$  is the standard deviation of  $B'_{i,y}$ . The cost function was calculated iteratively using a Nelder-Mead simplex optimisation method (Nelder and Mead, 1965) considering different combinations of the following four parameters: the daily mortality rate of eggs ( $Z_e$ , Eq. 1), the mortality rate of adults ( $Z_a$ , Eq. 1), the coefficient of natural mortality scaling the decrease in mortality with size ( $z$ , Eq. 1), and the slope of the density-dependent relationship between egg concentration and larval mortality ( $s$ , Eq. 2). The choice of these parameters for optimization was based on the difficulty of assessing mortality values in the field and the scarcity of the related literature.

As described above, our modelling approach allows to assess the impact of the mortality caused by winter starvation on the population ( $Z_{DEB}$ ). This parameter is often disregarded in fish population modelling due to the empirical difficulties of estimation. By running a simulation where this source of mortality is disregarded, we were able to highlight its relevance for the population, which can be seen as an added value of our work. To make a simulation with no death by starvation -making sense when compared to the base-case simulation- it was

necessary to consider a new calibration of the mortality parameters  $Z_a$ ,  $Z_e$ ,  $z$ , and  $s$ , in the same manner as described above.

## Model validation

The model validation consisted of the comparison of the model outputs to independent data from scientific surveys for the stock assessment. Acoustic surveys for the stock assessment of anchovy in the Bay of Biscay are carried out during PELGAS spring surveys by the Institut Français de Recherche pour l'Exploitation de la Mer, IFREMER (France) (Doray et al., 2018). A second dataset comes from BIOMAN spring surveys conducted by AZTI-Tecnalia (Spain), which use the daily egg production method (DEPM) for an independent stock assessment of anchovy in the Bay of Biscay. In the validation of our model both the number of individuals and their weight are taken into account to obtain the equivalent of the population SSB provided by the surveys. The outputs of our model were extracted in spring (May 15<sup>th</sup>) for comparison with these surveys. In order to obtain a statistical measurement of the model validation, we estimated the significance of the slope ( $H_0$ : slope = 0) from the linear regression between the model and both independent time series (PELGAS and BIOMAN).

## Hypotheses and scenarios

In order to study the separate effects of fishing mortality and environmental variables on population dynamics, different scenarios combining fishing pressure and environmental forcing were defined (Table 1). Scenarios were defined based on different hypotheses about the relationship between external forcing and population response. First, in order to show the effect of fishing, the interannual variability of the environment was disregarded and instead, a daily climatology of temperature and zooplankton computed over the period under study was used (Scenario 1). Similarly, to study the effect of the environment on the population, fishing mortality ( $Z_F$ ) was set constant (as the average of the whole time-series) over the full period of study (Scenario 2), or just during the fishing ban (Scenario 3), aiming at understanding the effects of fishing over the entire period and the consequences of the fishing ban between 2005 and 2010.

Our modelling approach can also test the effect of different harvest rates or control rules on the stock performance. The current harvest control rule (HCR) has been implemented since 2010 (ICES, 2018), and is used to define a total allowable catch (TAC, in tonnes) of anchovy in a given year in the Bay of Biscay. This TAC, implemented from January to December of year  $y+1$ , is calculated based on the SSB at the end of the first semester of year  $y+1$  as follows:

- $TAC_{y+1} = 0 \text{ t}$ ; if  $SSB_{y+1} \leq 24,000 \text{ t}$
- $TAC_{y+1} = -2,600 + 0.40 * SSB_{y+1}$ ; if  $24,000 \text{ t} < SSB_{y+1} \leq 89,000 \text{ t}$
- $TAC_{y+1} = 33,000 \text{ t}$ ; if  $SSB_{y+1} > 89,000 \text{ t}$

$SSB_{y+1}$  is estimated by the assessment group on December of year  $y$  based on a recruitment prediction for year  $y+1$ . As we cannot make this projection in our model, we calculate the TAC based on the modelled SSB on May 15<sup>th</sup> of the current year, and apply it from that date to the same date of the following year.

To include the HCR in the DEB-IBM model, it was necessary to translate it to an instantaneous mortality rate as  $Z_F$ . To do this, we extracted the SSB from our model on May 15<sup>th</sup> each year and the corresponding TAC was calculated according to the rules presented before. Then, using the average individual weight of adults and juveniles, we transformed the TAC into the number of individuals that can be captured (TAC') during the season, obtaining the instantaneous fishing mortality ( $Z_F$  in year<sup>-1</sup>) corresponding to the TAC' as:

$$Z_F = -\ln\left(\frac{N_m - TAC'}{N_m}\right) \quad \text{Eq. 5}$$

where  $N_m$  is the number of individuals on 15<sup>th</sup> May in the population. To investigate if the application of the HCR would have avoided the collapse of the population, we defined a scenario where this strategy was applied since 2000 (Scenario 4).

**Table 1.** Hypotheses on the influence of environment and fishing on the anchovy's population dynamics between 2000 and 2015, with scenarios proposed for testing them.

Hypothesis	Scenario
Hindcasted environmental variables and historical fishing mortality replicate the past dynamics of the population.	Sc0) Historical environmental forcing + historical fishing pressure.
Fishing pressure drives population dynamics.	Sc1) Historical fishing pressure + average environmental forcing (as daily climatology) in the period 2000-2015
Environmental variables drive population dynamics.	Sc2) Historical environmental forcing + constant fishing pressure.
The closure of the fishery was necessary for the recovery of the population.	Sc3) Historical environmental forcing + historical fishing pressure except between 2005 and 2010, when set constant.
The implementation of the current HCR in the beginning of the time series would have prevented the collapse of the population.	Sc4) Historical environmental forcing + HCR fishing pressure.

## Results

### Environmental variables

The environmental forcing variables used to run the model between 1996 and 2015 are shown in Figs. S1, S2, and S3. These figures also show the daily climatologies used for the calibration of the individual DEB and to run scenario 2, while in Fig. S4 a summary of four descriptors are shown for each year: annual mean temperature between 0 and 30 m, annual mean temperature between 0 and 150 m, annual mean zooplankton concentration, and the day of the year when the highest concentration of zooplankton occurs. Years 2003, 2014, and 2006 showed summer surface temperatures well over the daily 2000-2015 climatology (Figs. S1, S2, and S4). These years, except of 2006, presented also an earlier zooplankton bloom (Fig. S3), albeit the annual maximum could happen later in the year (Fig. S4). Year 2011 showed high spring temperature (Fig. S1), with an advanced zooplankton bloom (Figs. S3 and S4), but summer temperature was colder than the climatology. Years 2002, 2010, and 2013 were colder than the average in winter and spring, while no special feature was identified in zooplankton production during these years. (Figs. S1, S2, S3, and S4). No clear temporal patterns were found within the environmental forcing variables apart from an increasing mean zooplankton concentration (Fig. S4C,  $p\text{-val.}=0.0535$ ).

### Simulation at the individual level

The bioenergetic model captured successfully the dynamics of individual growth and energy density when using the daily 2000-2015 climatology as environmental forcing (Fig. S5, see also Gatti et al., 2017). Individual growth in weight and length, and energy density of individuals (see Gatti et al., 2017 for details on calculation) matched the observations from the surveys (dots in Fig. S5, see Gatti et al., 2017 for data origin). According to these simulations, individual length and weight reached an asymptote at around 18 cm and 37 g respectively. The model captured the variations in weight and energy density occurring on a seasonal scale based on the reproductive cycle and food availability.

### Reconstruction of the past population dynamics

The IDEB-IBM model was able to capture the main features of the population dynamics of the European anchovy between 2000 and 2015 in the Bay of Biscay (Fig. 3A). This includes the collapse of the population in 2005 and the recovery afterwards. Four parameters were optimized

(see methods): the daily adult mortality coefficient (Eq. 1,  $Z_a=0.000001$ ), the daily egg mortality coefficient (Eq. 1,  $Z_e=0.2494$ ), the coefficient parameterising length-decreasing natural mortality (Eq. 1,  $z=0.3491$ ), and the slope of the density-dependent mortality of larvae (Eq. 2,  $s=0.1418$ ). Similarly to the CBBM values, the biomass predicted by our model (Fig. 3A) decreased in the first few years of the simulation, with minimum values in 2005-2006 and two main drops in 2004 and 2007. After 2008, however, the population followed a steady and slow recovery until the end of the simulation, with a drop in 2014 (Fig. 3A). The regression between the simulated and CBBM biomass values is significant ( $r^2 = 0.40$ ; p-val. = 0.0039).

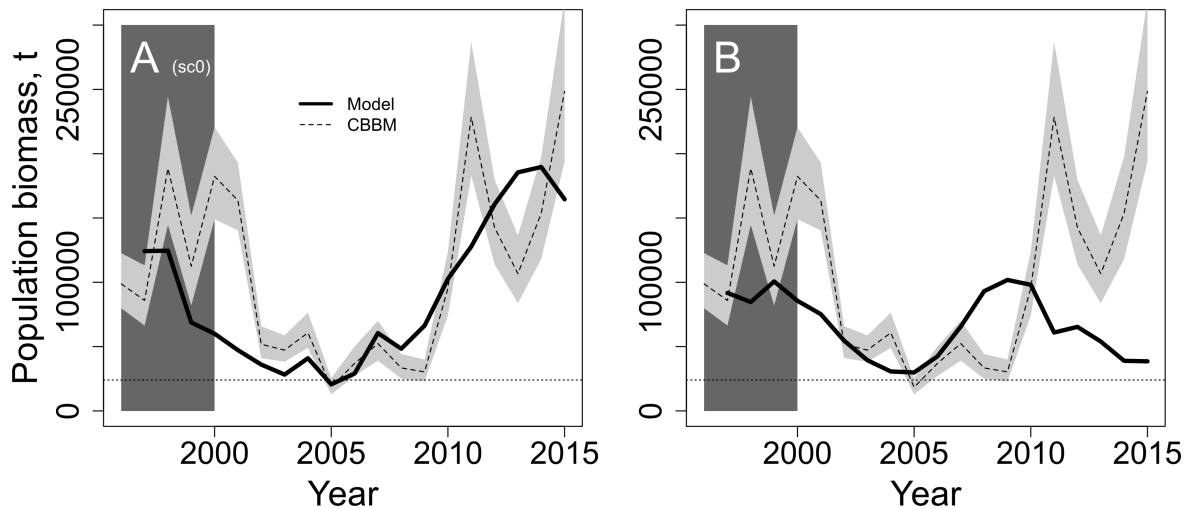


**Figure 3.** Model output (black solid line) for the biomass of anchovy in the Bay of Biscay on January 1<sup>st</sup>, considering the mortality by energetic failure within the DEB model ( $Z_{DEB}$ ) (panel A, scenario 0), and when this source of mortality is not considered (panel B). The dashed line represents the CBBM data with 95% confidence intervals (grey shadow). The dark background shows the spin-up period of the model (1996-1999), and the horizontal dotted line shows the 24,000 t limit stated by the HCR to close the fishery.

The model was validated using biomass and weight-at-age values from biomass estimation surveys PELGAS and BIOMAN (see methods). As on January 1<sup>st</sup> (Fig. 3A), the population biomass on May 15<sup>th</sup> reached a minimum in 2005 and recovered afterwards (Fig. 4A). A second important drop was also found in 2012. These dynamics are broadly coincident with the results from the research cruises, including the drop near the end of the time series (Fig. 4A). The regression between observations and the model outputs showed significant relations (p-val. = 0.020 PELGAS; p-val. = 0.0563 BIOMAN, although the fit was poor ( $r^2 = 0.327$  PELGAS;  $r^2 =$

0.236 BIOMAN) (Fig. 4B). Additionally, the weight-at-age on May 15<sup>th</sup> for the different ages in the population agreed with the survey data, albeit the interannual variability in the model outputs was lower (not shown).

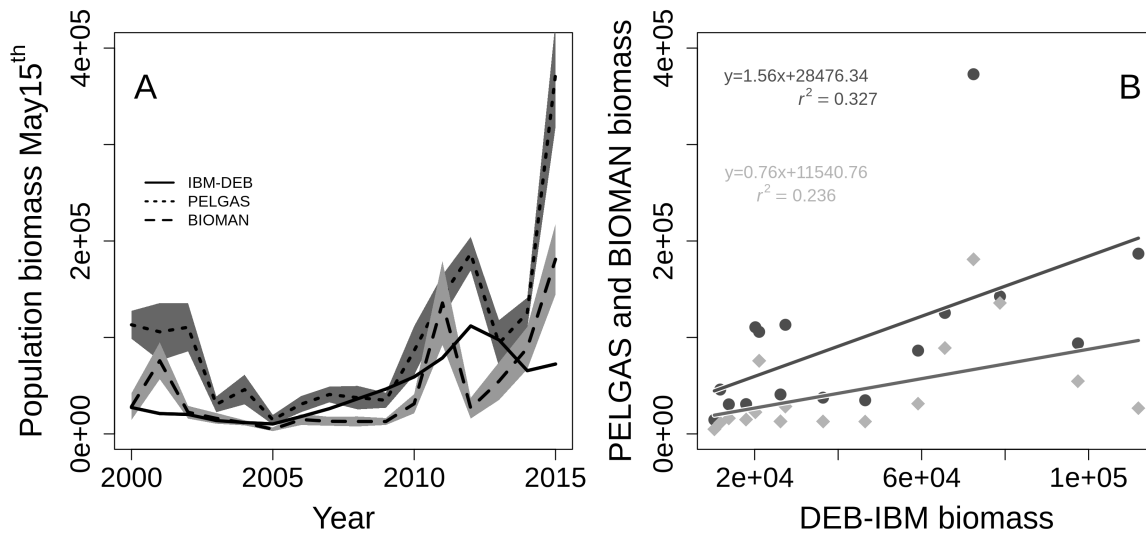


**Figure 4.** Model validation. A) Time series of population biomass (tonnes) on May 15<sup>th</sup>, with reference values from PELGAS (pointed line) and BIOMAN (dashed line), with 95% confidence intervals shown for both reference estimates. B) Linear regressions between model output and biomass reference values from PELGAS (dark grey) and BIOMAN (light grey).

From the DEB-IBM simulations, a variety of ecological indicators can be extracted to understand the mechanisms underlying the population dynamics (Fig. 5). The age-structure of the population in terms of number of individuals can be obtained at different times of the year. On 1<sup>st</sup> of January, the proportion of age 1 individuals was found to be around 80% (Fig. 5A), while on May 15<sup>th</sup> it decreased to around 50% (Fig. 5B). DEB-mortality, at the end of winter, is hence largely responsible for the loss of a high percentage of simulated age 1 individuals (Fig. 6), 2014 being the year with the highest drop in the proportion of age 1 individuals between January 1<sup>st</sup> and May 15<sup>th</sup> (Fig. 5B). This can be also appreciated in Fig. S7A and B, where the number of recruits on January 1<sup>st</sup> and May 15<sup>th</sup> is shown. Similarly, the age structure in terms of biomass (Fig. 5C, 1<sup>st</sup> of January), shows that age 1 individuals are not so dominant as in terms of numbers of individuals, and that the proportion corresponding to the different age classes did not vary significantly during the time series.



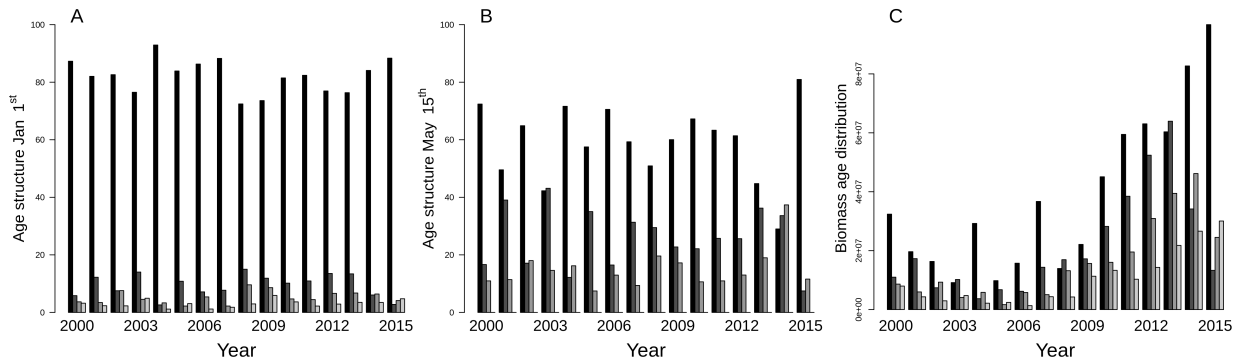


**Figure 5.** Ecological indicators obtained from the DEB-IBM model (I). A) Proportion, in number of individuals, of each age class on January 1<sup>st</sup>. B) Proportion, in number of individuals, of each age class on May 15<sup>th</sup>. C) Biomass distribution (tonnes) by age class on January 1<sup>st</sup>. The colours of the bars represent the different age classes: age 1, age 2, age 3, and age 4 from black to light grey.

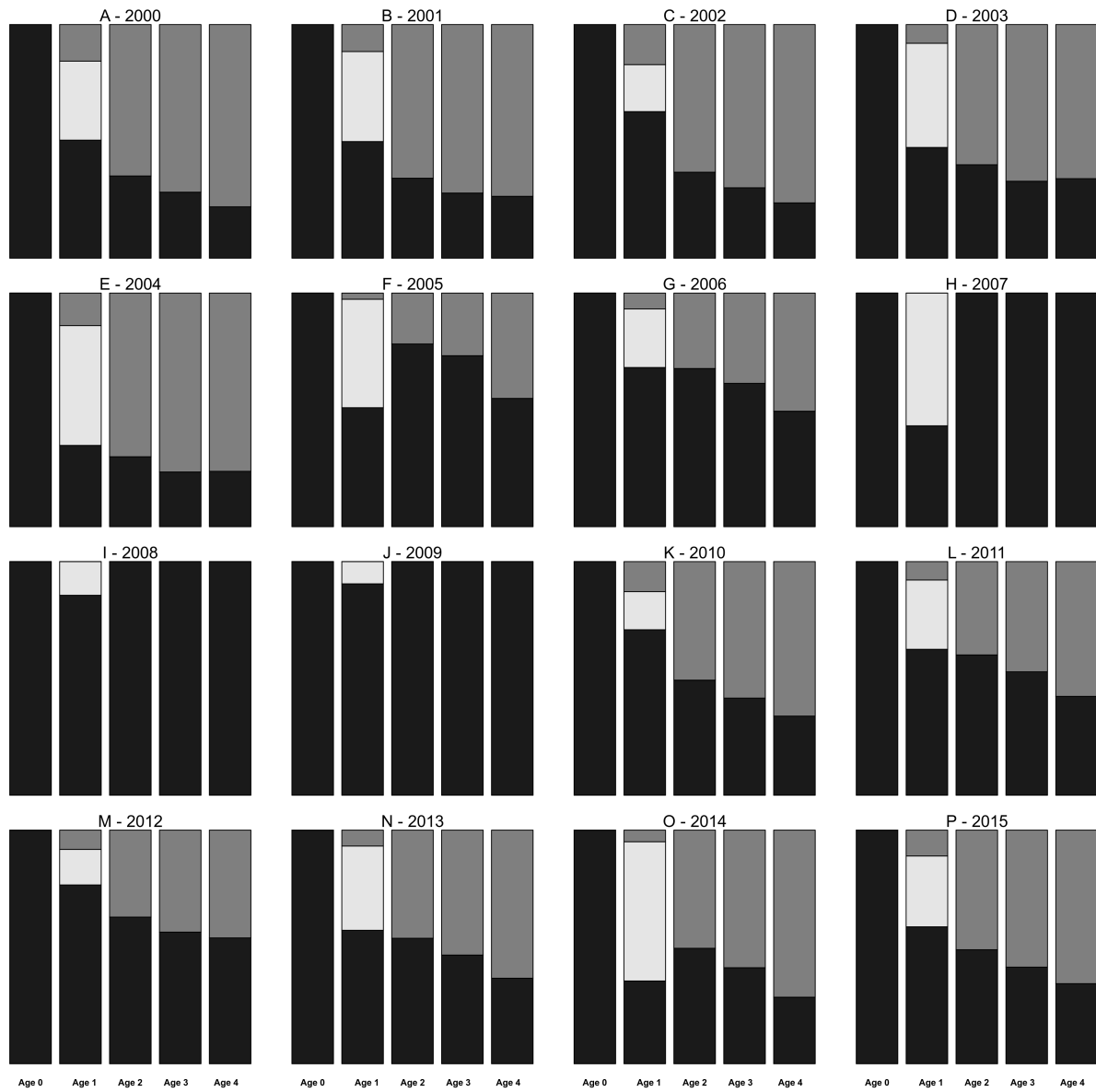


**Figure 6.** Ecological indicators obtained from the DEB-IBM model (II). Sources of mortality by age and year as a proportion of the total number of dead individuals of a given age and year during the simulation. Black: natural mortality; white: DEB mortality; grey: fishing mortality.

Different ecological indicators obtained from the DEB-IBM model show a drop in the performance of the population in 2004 (Fig. S7): egg survival, fertility, mean weight gain between January and May, Fulton's index as the condition factor, average adult weight, and the energy content of individuals in different DEB compartments. The energy density of age 1 individuals on January 1<sup>st</sup> did not show any special characteristic between 2004 and 2005, but dropped significantly in 2013 and 2014 (Fig. S7E). The average size at age did not vary significantly between 2000 and 2015 (Fig. S7H), with the highest inter-annual variation found for age 1.

The contribution of each source of mortality to the total mortality was estimated with the DEB-IBM model (Fig. 6). The starvation mortality ( $Z_{DEB}$ ) affected age 1 individuals only. It happens at the end of winter when the recruits have insufficient resources and therefore die. Fishing mortality ( $Z_F$ ) was more important than natural mortality for ages 2, 3, and 4, affecting age 1 as well. Natural mortality ( $Z_N$ ) decreases in importance as fishes grow (Fig. S6). Within the hindcasted period,  $Z_{DEB}$  was found to be especially high in 2004 and 2007. After 2008,  $Z_{DEB}$  dropped for age 1 individuals, until 2014 when it suffered a sudden increase.

The simulation where  $Z_{DEB}$  was not included in the DEB model (additional simulation, Fig. 3B) required a different calibration of the mortality parameters ( $Z_a = 0.0004$ ,  $z = 1.045$ ,  $Z_e = 0.950$ ,  $s=0.172$ ). In this simulation, the population was found to drop from the beginning of the period until 2005, recovering afterwards and dropping again by the end of the simulation (Fig. 3B). Part of the interannual variability was lost, and many indicators were substantially different from scenario 0 (Fig. S8). The proportion of individuals dying by fishing mortality was increased, while the energetic minima of 2004, 2007, and 2014 were also captured under this simulation.

## Fishing and climate scenarios

Following the scenarios approach shown in Table 1, applying a constant fishing mortality rate with the historical environmental forcing should demonstrate the real impact of environmental forcing alone (scenario 1; Fig. 7A). In this simulation, the population dropped during the first years but to a lower extent than when the real fishing mortality was applied (Fig. 3A and the grey line in Fig. 7A). Then, the population reached two minima, in 2003 and 2005, dropping again in 2008. At the end of the simulation the population did not increase as much as under scenario 0. The interannual variability was found to be higher in scenario 1 than in scenario 0 (Fig. 7A). Fig. S9 shows the different ecological indicators extracted from this simulation. The

age composition of the population was similar to scenario 0, while the recruitment was higher in the beginning of the time series, but lower in the end. The drop of indicators found in 2004 under scenario 0 was also found for the weight gain between January and May, the Fulton's condition factor, the egg survival, and the fecundity. According to the energetics of individuals, important drops were also registered in 2004, 2007, and 2014.

In scenario 2 (fishing alone drives population dynamics: Table 1, Fig. 7B) the population was found to suffer a drastic increase after the closure of the fishery in 2005, stabilizing at the end. The interannual variability was found to be much lower than in scenarios 0 and 1, which is also evident in a range of ecological indicators (Fig. S10). The drop of performance found in scenarios 0 and 1 in 2004 was not so evident, but still present in this scenario, mainly referring to the Fulton's condition factor and the fecundity of individuals, while the survival of eggs decreased by the end of the simulation (Fig. S10 G, I, J).

Under scenario 3 (closure necessary for the recovery: Table 1, Fig. 7C), the population did not recover after the collapse of 2005, keeping minimal values until the end of the simulation. Ecological indicators showed the same patterns as in scenario 0, but with lower values by the end of the simulation. This is especially evident for the recruitment and for the proportion of age 1 individuals in terms of numbers and biomass (Fig. S11).

The simulation of the application of the current HCR from the beginning of the period (scenario 4), showed that the population did not drop at the beginning, being sustained well over the limit of 24,000 tonnes established in the HCR to close the fishery (Fig. 7D). The interannual variability was found to be coincident with scenarios 0, 1, and 3, while the final period, on the other hand, did not show the increase in population found in the scenario 0 simulation: instead, it was more or less stable around 100,000 tonnes. Ecological indicators also show similar patterns as those for scenario 1, with drops of individual performance in 2004, 2007, and 2014 and with lower recruitment values in 2003, 2005, 2008, and 2012 (Fig. S12).

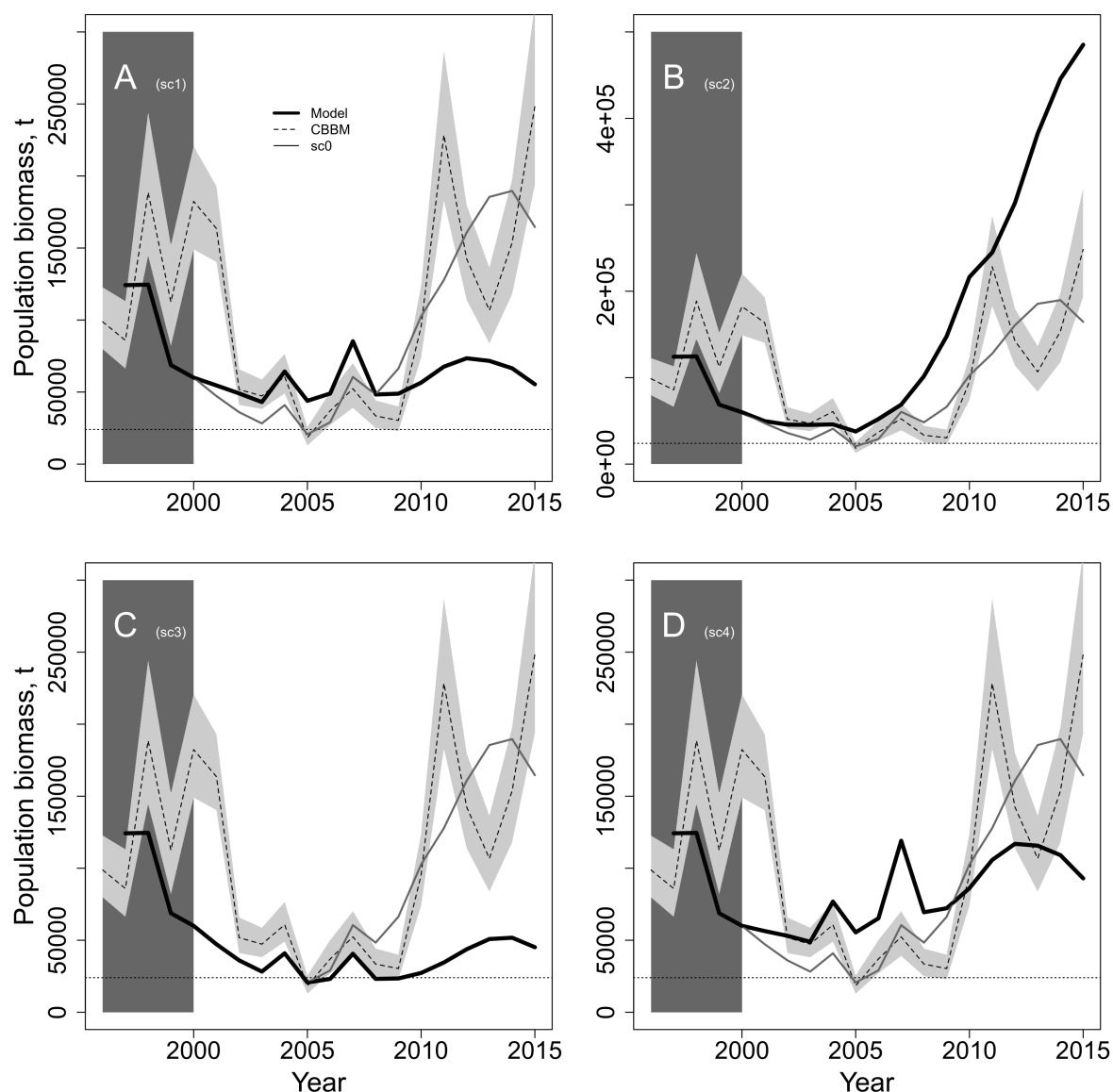


**Figure 7.** Model output (black solid line) for the biomass of anchovy in the Bay of Biscay on January 1<sup>st</sup>, using the different environmental and fishing scenarios described in Table 1: A) constant fishing mortality at the average of the time series, with historical environmental forcing (scenario 1); B) historical fishing mortality with constant environmental forcing as a daily climatology repeated year after year (scenario 2); C) historical environmental forcing and fishing pressure, but assuming constant fishing mortality at the average of the time series between 2005 and 2010 (scenario 3); D) implementation of the HCR since 2000 (scenario 4). The continuous grey line shows the population biomass from scenario 0 (Fig. 3A) for comparison. The dashed line represents the CBBM data with 95% confidence intervals (grey shadow). The dark background shows the spin-up period of the model (1996-1999), and the horizontal dotted line shows the 24,000 t limit stated by the HCR to close the fishery.

## Discussion

492 We integrated for the first time a bioenergetics model into a population model for the Bay of  
Biscay anchovy. This coupling framework successfully replicated the main patterns of the  
494 population dynamics between 2000 and 2015 (Fig. 3A), including the initial drop, the collapse of  
2005, and the recovery after 2008. Additionally, by combining this approach with simulations  
496 based on different scenarios of environmental and fishing pressure, we provide new insights  
into the causes of the collapse of 2005 and on the recovery afterwards. Our results provide  
498 evidence that the interannual variability of the anchovy population was mostly driven by  
environmental conditions, while the effect of fishing was more evident on a longer time scale.  
500 We also investigated the relevance of the closure of the fishery between 2005 and 2010 for the  
recovery of the population, as well as the likely consequences of the implementation of the  
502 current HCR before the collapse.

504 Including the effect of mortality associated with individual bioenergetics improved the hindcast  
ability of the model (Fig. 4A vs 4B). The calibration considering  $Z_{DEB}$  (scenario 0; Fig. 3A)  
506 provided estimates of egg ( $Z_e$ ), and adult ( $Z_a$ ) mortality rates consistently lower than values in  
the literature (Uriarte et al., 2016). This result was expected as natural mortality measured in the  
508 literature should be comparable to the sum of  $Z_{DEB}$  and  $Z_N$  in our modelling framework. On the  
other hand, the values of  $Z_a$  and  $Z_e$  when  $Z_{DEB}$  was not taken into account (Fig. 3B) were much  
510 higher. Further, the interannual variability was better captured when  $Z_{DEB}$  was considered. This  
source of mortality could be very important for the recruitment success at the end of the first  
512 winter as it affects age 1 individuals. A negative (but non-significant) relationship between the  
number of recruits on May 15<sup>th</sup> and the proportion of dead individuals by  $Z_{DEB}$  in the previous  
514 winter (both estimated from our model) was found ( $p\text{-val.}=0.091$ ;  $r^2=0.19$ ). Hence, according to  
our results, this potential source of mortality establishes a direct link between the environmental  
516 variability and the resulting population dynamics. Due to inherent methodological difficulties, few  
references on natural mortality by starvation during winter for early stages of pelagic fish are  
518 available (but see Pepin, 2015a, 2015b).

520

## Population dynamics related to environmental and fishing

Simulating the anchovy population under different scenarios (Table 1) allowed us to study the effects of fishing and environment on the population dynamics. Hence, while scenario 1 (population subject to constant fishing mortality, Fig. 7A) captured the interannual variability of the simulation of reference, it failed to replicate the drop and recovery of the population. On the other hand, under scenario 2 (no interannual variability of the environment, Fig. 7B) the simulation did not capture the interannual variability of the population, but rather, the longer-term pattern of increase-decrease in biomass. These findings suggest a short-term control of the population by environmental drivers, while the effect of fishing would have effect on a longer time scale. This is probably because of the autorreccorrelation of the fishing pressure showing a clear temporal trend: high at the beginning of the simulation, minimal or null between 2005 and 2010, and intermediate between 2010 and 2015. In fact, the response of the population to the closure of the fishery under scenario 2 (constant environment) was immediate in 2005, demonstrating that fishing pressure could affect population dynamics in a short temporal scale as well.

Scenarios 1 (constant fishing) and 2 (constant environment) suggest a joint action of environmental and fishing on the drop and collapse of the population in the early 2000s. Hence, scenario 1 (and scenario 4, see below) showed that environment was unfavourable for the population during that period, and also, that a lower fishing mortality at the beginning of the time series would have prevented the collapse of the population (Fig. 7A). On the other hand, the constant environment simulated in scenario 2 indicated that fishing pressure alone was sufficient to cause a low population before 2005, close to the 24,000 t limit established by the HCR to close the fishery (Fig. 7B). The corollary of these simulations is that both factors contributed to the fall of the population, with the especially bad environmental conditions of 2004 being the definitive drivers of the collapse of the population in 2005 (see below a mechanistic discussion on the specific causes). This finding is in agreement with the work of Taboada and Anadón (2016), which showed that fishing pressure was fundamental to explaining the collapse of the population in 2005, in addition to environmental variables such as the phytoplankton bloom phenology or the larval drift.

In a similar manner, the recovery of the population after 2008 in our model was probably triggered by a combination of low fishing pressure and favourable environmental conditions. Fig. 6 showed that the recovery period of the simulation had the lowest proportion of  $Z_{DEB}$  of the time

series, while the simulation of scenario 4 (with no closure of the fishery; Fig. 7D), demonstrated that the population would not have been able to recover if fishing had been kept constant between 2005 and 2010. Interestingly, as shown in the simulation of scenario 1 (constant fishing), the effect of lower  $Z_{DEB}$  would have not been sufficient to trigger the recovery of the population (Fig. 7A), probably due to an increased fishing mortality in regards of scenario 0. By contrast, the closure of the fishery alone (scenario 2) would probably have been enough to allow the recovery of the population (Fig. 7B) which, comparing with scenario 0, could have been faster than under variable environmental forcing. Hence, both the closure of the fishery and the drop of  $Z_{DEB}$  were beneficial and coincident in time for the population, finally triggering its recovery. The environmental causes of the drop of  $Z_{DEB}$  in this period are discussed below.

### Mechanistic perspective of the population dynamics

The environmental features preceding the collapse of 2005 deserve special consideration to understand the mechanisms of action of environmental variables on the bioenergetics of individuals and populations. 2003 temperature was significantly high at both 0-30 and 0-150 m integrated depths (Figs. S1, S2) with an early bloom of zooplankton in spring and low zooplankton concentration during the second part of the year (Fig. S3), while in 2004 temperature and zooplankton concentration were close to the average (Figs. S1, S2, S3). As a consequence of the higher temperature, different indicators extracted from our model on January 1<sup>st</sup> 2004 indicate good individual performance during 2003: a higher proportion of the time series of age 1 individuals (Fig. 5A), high proportion of age 1 individuals in terms of biomass (Fig. 5C), high recruitment of individuals (Fig. S7A), age 1 individuals with high energy density (Fig. S7E), and large adults (Fig. S7I), with high energy levels (Fig. S7J). Conversely, indicators from the model obtained on May 15<sup>th</sup> 2004 show a trend change, with the lowest weight gain between January and May (Fig. S7C), and a critical drop of energetics between 2003 and 2004 (Fig. S7J). The drop of performance at the individual and population level is also in agreement with the high  $Z_{DEB}$  (Fig. 6) shown by the model. This mortality is expected to take place at the end of winter when individuals cannot pay maintenance costs from food or from reserves.

The high and low performance of the modelled population in 2003 and 2004 respectively can probably be explained from a bioenergetics perspective. The high temperature in 2003 contributed positively to the growth and reproduction of individuals in our model. Yet, despite many indicators showing good performance of the population at the beginning of 2004, the



lower food during the second part of 2003 was the reason why age 1 individuals and adults showed low energy density in 2003 (Figs. S7E). This led to insufficient accumulation of reserves to face the winter and caused the drastic drop of energy observed between 2003 and 2004 (Fig. S7J). Furthermore, the high temperature of 2003 and the early zooplankton bloom could have favoured the growth of individuals in the first half of 2003, with a consequent increase of maintenance costs at the individual level (proportional to body volume). In this sense, the model predicts a trade-off along the size spectra, with lower predation-based mortality for bigger individuals but also higher risk to starve. This could make the population especially sensitive to subsequent 2003-2004 winter scarcity of food and explain the lowest-in-the-time-series weight gain as well as high bioenergetics mortality ( $Z_{DEB}$ ) at age 1 between January and May 2004 (Fig. S7C). All these phenomena, together with the lowest fecundity of the time series in 2004 as a consequence of the low food in the second part of 2003 (Fig. S7G), led to the collapse of the population in 2005.

After 2005, several indicators showed positive trends for the recovery of the population. The proportion of individuals dying because of energetic failure ( $Z_{DEB}$ ) in 2006 dropped and stayed low until 2012 (Fig. 6), except for 2007. These years were warm in general (Figs. S1, S2, S4), and with zooplankton in late autumn (Fig. S3), resulting in shortening of the winter period and thus decreasing starvation risk. In 2013  $Z_{DEB}$  rose again, which coincided with a delay in the bloom of zooplankton resulting in food scarcity at the end of winter, increasing the mortality of age 1 individuals by starvation. This truncated the recovery of the modelled population between 2013 and 2014 according to our simulation. The observations from the CBBM, on the other hand, showed drastic drops of the biomass in 2011 and 2012. None of our simulations captured these features, but it is worth noting that CBBM estimates may be subject to considerable error as well.

### Retrospective application of the HCR

One of the consequences of the closure of the fishery between 2005 and 2010 was the subsequent implementation of the HCR to estimate the TAC of anchovy in the Bay of Biscay. This measure established a lower SSB boundary of 24,000 tonnes to close the fishery and a maximal catch of 33,000 tonnes if the estimated SSB was higher than 89,000 tonnes (see Materials and methods and Sánchez et al., 2019 for a deeper analysis of the HCR). Simulating this HCR from the beginning of the period is a direct application of the DEB-IBM approach, and is useful for evaluating the utility of this policy to prevent the collapse of the population. Also, it

permits us to analyse whether the upper TAC limit of 33,000 tonnes is sufficiently restrictive to avoid situations of risk for the population. In this manner, under scenario 4, we found that the biomass of the population remained well over the lower boundary of 24,000 tonnes during the whole simulation (Fig. 7D), and also, that the biomass minimum occurred in 2003, after which the population started to increase slightly. This result shows that the current HCR could be adequate to avoid the collapse of the population under similar circumstances, but also showed that the population would have been impeded from growing as much as under scenario 0, where the closure of the fishery for five years was pivotal for the increase of the population to current values of around 150,000 tonnes (Fig. 3A).

### Model limitations and sensitivity analysis

The integrated DEB-IBM model presented here contains inherent noise related to model parametrization and estimated parameters. At the individual level, the genetic inter-individual variability within the population was not considered, instead the unique determinant of the individual life history trajectory and phenotype was the environmental conditions from the birth date. Also, the model is constructed based on more than 20 parameters within the IBM and DEB modules that are subject to estimation errors (see Gatti et al., 2017). These parameters were calibrated in regards of individual size, weight-at-age, seasonal data on energy density, and yearly time-series of population biomass which further introduced some error. The overall error associated with the calibration of our mortality parameters is difficult to assess since the CBBM biomass time-series used as reference is an estimation from an assessment model containing its own intrinsic uncertainties (Ibaibarriaga et al., 2008). The density-dependent mortality ( $Z_{DD}$ ), only applied to the larval stage in our model, likely affects juveniles and adults as well, introducing more error in the estimations of mortality. The initialization parameters used for the population in 1996 were also obtained from surveys (see Gatti et al., 2017), being subject to estimation errors as commented before and introducing some noise into the model as well. Initialization parameters always influence simulations, and the purpose of this work was to use the most realistic set of initial conditions available from data. Hence, we considered the population structure and energetics respectively from the surveys (see Gatti et al., 2017) and the individual run with climatological forcing (Fig. S5) as reliable data for initialization. Minor adjustments in DEB parameters ( $p_{Am}$  and  $K$ ) relative to the work of Gatti et al. (2017) were applied in order to stabilize the population during the spin-up period. These parameters were chosen because they had the highest uncertainty of estimation. The stabilization of the population during the spin-up period was measured in terms of the number of SIs conforming

the population (around 130), but still there was an important gap between the modelled population biomass and CBBM data in 2000.

At the population level the model is not spatially explicit, which means that all the environmental variables are averaged over the area of study (Fig. 1). This limits the effectiveness of the model because spatial processes, such as the variability in spatial distribution throughout the life cycle, or variability in larval drift, may explain part of the unresolved variability between the observations and the historical evolution of the population. In any case, it is also worth to mention that while new model components such as spatial detail, or individual variability, could increase the resolution of the model, they could also make predictions more uncertain if poorly parameterized. Furthermore, the outputs from the physical-biogeochemical model providing environmental data (POLCOMS-ERSEM) contain their own sources of error. Improving both aspects in our model (individual variability and spatial detail) seems to be necessary to increase the resolution of the model, whereas they could lead to more uncertain predictions if poorly parameterized.

Finally, a sensitivity analysis was carried out in order to determine the importance of variations of the considered environmental variables on the behaviour of the DEB-IBM model. This consisted of simulations of population biomass evolution under conditions of increased/decreased zooplankton concentration and temperature (Fig. S13). Generally, the response of the population was found to be favoured both by increased temperature and increased zooplankton, which could be understood from a bioenergetics perspective of metabolic enhancement leading to improved individual performance.

## Conclusions

This is the first time that a bioenergetics model for the Bay of Biscay anchovy has been coupled to an IBM with the purpose of hindcasting the period of the population collapse and recovery at the beginning of the century. Our modelling approach allowed us to study the effect of the environmental and human pressures on the population of anchovy, and showed that the environmental variability had immediate consequences on the population dynamics, while the effect of the fishery was apparent on a longer temporal scale. Moreover, the collapse of the population seems to have been a joint consequence of an elevated fishing pressure in the years preceding the collapse and unfavourable environmental conditions in the year before the

collapse, with an exceptionally long winter (leading to food scarcity) causing a great natural  
688 mortality due to starvation. In the same manner, the recovery of the population was mainly  
triggered by the closure of the fishery for 5 years and favoured by warmer years with short  
690 winters leading to the appearance of larger individuals with high fecundity. Finally, a simulation  
of a retrospective implementation of the current HCR showed that this measure could have  
692 avoided the collapse of the population and the closure of the fishery in 2005.

## Acknowledgements

694 This work was funded by the CERES project, which has received funding from the European  
Union's Horizon 2020 research and innovation programme under grant agreement No 678193.

## 696 Bibliography

- 698 - Allain, G., Petitgas, P., Lazure, P. 2001. The influence of meso-scale ocean processes  
on anchovy (*Engraulis encrasicolus*) recruitment in the Bay of Biscay estimated using a  
3D hydrodynamic model. Fisheries Oceanography 10: 151-163.
- 700 - Allain, G., Petitgas, P., Lazure, P., Grellier, P. 2007. Biophysical modelling of larval drift,  
growth and survival for the prediction of anchovy (*Engraulis encrasicolus*) recruitment in  
702 the Bay of Biscay (NE Atlantic). Fisheries Oceanography 16: 489-505.
- Borja, A., Fontán, A., Sáenz, J., Valencia, V. 2008. Climate, oceanography, and  
704 recruitment: the case of the Bay of Biscay anchovy (*Engraulis encrasicolus*). Fisheries  
Oceanography 17: 477-493.
- 706 - Butenschön, M., Clark, J., Aldridge, J. N., Allen, J. I. Artioli, Y., Blackford, J., et al. 2016.  
ERSEM 15.06: a generic model for marine biogeochemistry and the ecosystem  
708 dynamics of the lower trophic levels. Geosciences Model Developments 9: 1293-1339.
- Checkley, D., Alheit, J., and Oozeki, Y. 2009. Climate change and small pelagic fish. Ed:  
710 Alheit, J. and Oozeki, Y.
- Cotano, U., Irigoien, X., Etxebeste, E., Álvarez, P., Zarauz, L., Mader, J., Ferrer, L. 2008.  
712 Distribution, growth and survival of anchovy larvae (*Engraulis encrasicolus* L.) in relation  
to hydrodynamic and trophic environment in the Bay of Biscay. Journal of Plankton  
714 Research, 30: 467-481.
- Cury, P., Bakun, A., Crawford, R.J.M., Jarre, A., Quiñones, R.A., Shannon, L.J.,  
716 Verheye, H.M. 2000. Small pelagics in upwelling systems: patterns of interaction and  
structural changes in “wasp-waist” ecosystems. ICES Journal of Marine Sciences 57,  
718 603–618.
- Dee, D. P., Uppala, S. M., Simmons, A.J., Berrisford, P., Poli, P., Kobayashi, S., Andrae,  
720 U., Balmaseda, M. A., Balsamo, G., Bauer, P., Bechtold, P., Beljaars, A. C. M., van de  
Berg, L., Bidlot, J., Bormann, N., Delsol, C., Dragani, R., Fuentes, M., Geer, A. J.,  
722 Haimberger, L., Healy, S. B., Hersbach, H., Hólm, E. V., Isaksen, L., Kållberg, P.,  
Köhler, M., Matricardi, M., McNally, A. P., Monge-Sanz, B. M., Morcrette, J.-J., Park, B.-

- 724 K., Peubey, C., de Rosnay, P., Tavorato, C., Thépaut, J.-N., Vitart, F. 2011. The ERA-  
 726 Interim reanalysis: configuration and performance of the data assimilation system.  
 Quarterly Journal of the Royal Meteorological Society 137, 553–597.
- Doray, M., Petitgas, P., Romagnan, J. B., Huret, M., Duhamel, E., Dupuy, C., Spitz, J. et  
 728 al. 2018. The PELGAS survey: ship-based integrated monitoring of the Bay of Biscay  
 pelagic ecosystem. Progress in Oceanography 166: 15-29.
  - Fietcher, J., Rose, K. A., Curchitser, E. N., Hedstrom, K. S. 2015. The role of  
 730 environmental controls in determining sardine and anchovy population cycles in the  
 732 California Current: Analysis of an end-to-end model. Progress in Oceanography 138:  
 381-398.
  - Gatti, P., Petitgas, P., Huret, M. 2017. Comparing biological traits of anchovy and  
 734 sardine in the Bay of Biscay: A modelling approach with the Dynamic Energy Budget.  
 736 Ecological Modelling 348: 93-109.
  - Gatti, P., Cominassi, L., Duhamel, E., Grellier, P., Le Delliou, H., Le Mestre, S., Petitgas,  
 738 P., Rabiller, M. Spitz, J. and Huret, M. 2018. Bioenergetic condition of anchovy and  
 sardine in the Bay of Biscay and English Channel. Progress in Oceanography 166: 129-  
 740 138.
  - Holt, J. T., James, I. D., Jones, J. E. 2001. An s coordinate density evolving model of the  
 742 northwest European continental shelf 1, Model description and density structure. Journal  
 of Geophysical Research, 105: 14015-14034.
  - Huret, M., Bourriau, P., Gatti, P., Dumas, F., Petitgas, P., 2016. Size, permeability and  
 744 buoyancy of anchovy (*Engraulis encrasicolus*) and sardine (*Sardina pilchardus*) eggs in  
 746 relation to their physical environment in the Bay of Biscay. Fisheries Oceanography 25:  
 582-597.
  - Huret, M., Tsiaras, K., Daewel, U., Skogen, M. D., Gatti, P., Petitgas, P., and Somarakis,  
 748 S. 2018. Variation in life-history traits of European anchovy along a latitudinal gradient: a  
 750 bioenergetics modelling approach. Marine Ecology Progress Series.  
<https://doi.org/10.3354/meps12574>.
  - Huse, G, Giske, J., Salvanes, A. G. V. 2002. Individual-based models. Chapter in  
 752 Handbook of fish biology and fisheries. Vol. 2. Blackwell Science Ltd.
  - Ibaibarriaga, L., Fernández, C., Uriarte, A., Roel, B. A. 2008. A two-stage biomass  
 754 dynamic model for Bay of Biscay anchovy: a Bayesian approach. ICES Journal of  
 756 Marine Science, 65: 191-205.
  - ICES. 2018. Report of the Working Group on Southern Horse Mackerel, Anchovy and

758 Sardine (WGHANSA), 26-30 June 2018, Lisbon, Portugal. ICES CM 2018/ACOM:17.  
607 pp.

760 - Irigoien, X., Fernandes, J. A., Grosjean, P., Denis, K., Albaina, A., Santos, M. 2009.  
Spring zooplankton distribution in the Bay of Biscay from 1998 to 2006 in relation with  
762 anchovy recruitment. *Journal of Plankton Research* 31: 1-17.

- Jakobsen, T.; Fogarty, M. J.; Megrey, B. A. 2009. Fish reproductive biology implications  
764 for assessment and management. Ed. Wiley.

- Kooijman, S. 2010. Dynamic Energy Budget Theory for Metabolic Organisation, third  
766 edition, Cambridge University Press.

- Letcher, B. H., Rice, J. A., Crowder, L. B., and Rose, K. A. 1996. Variability in survival of  
768 larval fish: disentangling components with generalized individual-based model. *Canadian  
Journal of Fisheries and Aquaculture Science* 53: 787-801.

770 - Mayorga, E., Seitzinger, S.P., Harrison, J.A., Dumont, E., Beusen, A.H.W., Bouwman,  
A.F., Fekete, B.M., Kroeze C., Van Drecht G. 2010. Global Nutrient Export from  
772 WaterSheds 2 (NEWS 2): Model development and implementation. *Environmental  
Modelling and Software* 25: 837-853.

774 - Motos, L. 1996. Reproductive biology and fecundity of the Bay of Biscay anchovy  
population (*Engraulis encrasicolus* L.). *Scientia Marina* 60: 195–207.

776 - Nelder, J. A., and Mead, R. 1965. A simplex method for function minimization. *Computer  
Journal* 7: 308-313.

778 - Palomera, I., Olivar, M. P., Salat, J., Sabatés, A., Coll, M., García, A., Morales-Nin, B.  
2007. Small pelagic fish in the NW Mediterranean Sea: an ecological review. *Progress in  
780 Oceanography* 74: 377-396.

- Pepin, P. 2015a. Reconsidering the impossible-linking environmental drivers to growth,  
782 mortality, and recruitment of fish. *Canadian Journal of Fisheries and Aquatic Sciences*  
73: 205-215.

784 - Pepin, P. 2015b. Death from near and far: alternate perspectives on size-dependent  
mortality in larval fish. *ICES Journal of Marine Sciences* 73: 196-203.

786 - Pethybridge, H., Roos, D., Loizeau, V., Pecquerie, L., and Bacher, C. 2013. Responses  
of European anchovy vital rates and population growth to environmental fluctuations:  
788 and individual-based modelling approach. *Ecological Modelling* 250: 370-383.

- Plounevez, S., Champalbert, G. 1999. Feeding behaviour and trophic environment of  
790 *Engraulis encrasicolus* (L.) in the Bay of Biscay. *Estuarine, Coastal and Shelf Science*  
49: 177-191.

- 792 - Politikos, D. V., Somarakis, S., Tsiaras, K. P., Giannoulaki, M., Petihakis, G., Machias,  
794 A., and Triantafyllou, G. 2015 (a). Simulating anchovy's full life cycle in the northern  
Aegean Sea (eastern Mediterranean): a coupled hydro-biogeochemical-IBM model.  
Progress in Oceanography 138: 399-416.
- 796 - Politikos, D. V., Huret, M., Petitgas, P. 2015 (b). A coupled movement and bioenergetics  
798 model to explore the spawning migration of anchovy in the Bay of Biscay. Ecological  
Modelling 313: 212-222.
- Politikos, D. V., Curchitser, E. N., Rose, K. A., Checkley, D. M. Jr. Fiechter, J. 2018.  
800 Climate variability and sardine recruitment in the California Current: a mechanistic  
analysis of an ecosystem model. Fisheries Oceanography 27: 602-622.
- 802 - Prouzet, P., Uriarte, A., Villamor, B. Artzruoni, M., Gavrart, O., Albert, E., Biritxinaga, E.  
1999. Estimations de la mortalité par pêche (F) et naturelle (M) à partir des méthodes  
804 directes d'évaluation de l'abondance chez les petits pélagiques. Précision des  
estimateurs. Rapport final du contract européen 95/PRO/018.
- 806 - Rose, K. A., Cowan, J. H. Jr, Clark, M. E., Houde, E. D., Wang, S-B. 1999. An individual-  
based model of bay anchovy population dynamics in the mesohaline region of  
808 Chesapeake Bay. Marine Ecology Progress Series 185: 113-132.
- Rose, K. A., Fiechter, J., Curchitser, E. N., Hedstrom, K., Bernal, M., Creekmore, S.,  
810 Haynie, A., Ito, S. I., Lluch-Cota, S., Megrey, B. A., Edwards, C. A., Checkley, D.,  
Koslow, T., McClatchie, S., Werner, F., MacCall, A., and Agostini, V. 2015.  
812 Demonstration of a fully coupled end-to-end model for small pelagic fish using sardine  
and anchovy in the California Current. Progress in Oceanography Part B 138: 348–380.
- 814 - Sánchez, S., Ibaibarriaga, L., Uriarte, A., Prellezo, R., and others (2019) Challenges of  
management strategy evaluation for small pelagic fish: the Bay of Biscay anchovy case  
816 study. Marine Ecology Progress Series 617-618: 245-263.
- Scheffer, M., Baveco, J., DeAngelis, D., Rose K. and van Nes, E. 1995. Super-  
818 individuals: a simple solution for modelling large populations on an individual basis,  
Ecological Modelling 80: 161–170.
- 820 - Somarakis, S., Palomera, I., García, A., Quintanilla, L., Koutsikopoulos, C., Uriarte, A.,  
Motos, L. 2004. Daily egg production of anchovy in European waters. ICES Journal of  
822 Marine Science 61: 944-958.
- Somarakis, S., Nikolioudakis, N. 2007. Oceanographic habitat, growth and mortality of  
824 larval anchovy (*Engraulis encrasicolus*) in the northern Aegean Sea (eastern  
Mediterranean). Marine Biology 152: 1143-1158.



- 826 - Taboada, F. G., and Anadón, R. 2016. Determining the causes behind the collapse of a  
small pelagic fishery using Bayesian population modelling. *Ecological Applications*, 26:  
828 886-898.
- 830 - Uriarte, A., Ibaibarriaga, L, Pawlowski, L, Masse, J., Petitgas, P, Santos, M., Skagen, D.  
2016. Assessing natural mortality of Bay of Biscay anchovy from survey population and  
biomass estimates. *Canadian Journal of Fisheries and Aquatic Sciences* 73: 216-234.
- 832 - Vermard, Y., Marchal, P., Mahévas, S., and Thébaud O. 2008. A dynamic model of the  
Bay of Biscay pelagic fleet simulating fishing trip choice: the response to the closure of  
834 the European anchovy (*Engraulis encrasicolus*) fishery in 2005. *Canadian Journal of  
Fisheries and Aquatic Sciences* 65: 2444-2453.